ORIGINAL ARTICLE

Journal of Neurochemistry | JNC | WILEY

Preferential clustering of microglia and astrocytes around neuritic plaques during progression of Alzheimer's disease neuropathological changes

Wangchen Tsering[1,2,3] ⓘ | Ana de la Rosa[1] | Isabelle Y. Ruan[1] | Jennifer L. Philips[1,4] | Tim Bathe[1,4] ⓘ | Jonathan A. Villareal[1,4] ⓘ | Stefan Prokop[1,3,4,5] ⓘ

[1]Center for Translational Research in Neurodegenerative Disease, College of Medicine, University of Florida, Gainesville, Florida, USA

[2]Department of Neuroscience, College of Medicine, University of Florida, Gainesville, Florida, USA

[3]McKnight Brain Institute, College of Medicine, University of Florida, Gainesville, Florida, USA

[4]Department of Pathology, College of Medicine, University of Florida, Gainesville, Florida, USA

[5]Norman Fixel Institute for Neurological Diseases, University of Florida, Gainesville, Florida, USA

Correspondence
Stefan Prokop, Center for Translational Research in Neurodegenerative Disease, College of Medicine, University of Florida, Gainesville, FL, USA.
Email: sprokop@ufl.edu

Abstract

Neuroinflammation plays an important role in the pathological cascade of Alzheimer's disease (AD) along with aggregation of extracellular amyloid-β (Aβ) plaques and intracellular aggregates of tau protein. In animal models of amyloidosis, local immune activation is centered around Aβ plaques, which are usually of uniform morphology, dependent on the transgenic model used. In postmortem human brains a diversity of Aβ plaque morphologies is seen including diffuse plaques (non-neuritic plaques, non-NP), dense-core plaques, cotton-wool plaques, and NP. In a recent study, we demonstrated that during the progression of Alzheimer's disease neuropathologic changes (ADNC), a transformation of non-NP into NP occurs which is tightly linked to the emergence of cortical, but not hippocampal neurofibrillary tangle (NFT) pathology. This highlights the central role of NP in AD pathogenesis as well as brain region-specific differences in NP formation. In order to correlate the transformation of plaque types with local immune activation, we quantified the clustering and phenotype of microglia and accumulation of astrocytes around non-NP and NP during the progression of ADNC. We hypothesize that glial clustering occurs in response to formation of neuritic dystrophy around NP. First, we show that Iba1-positive microglia preferentially cluster around NP. Utilizing microglia phenotypic markers, we furthermore demonstrate that CD68-positive phagocytic microglia show a strong preference to cluster around NP in both the hippocampus and frontal cortex. A similar preferential clustering is observed for CD11c and ferritin-positive microglia in the frontal cortex, while this preference is less pronounced in the hippocampus, highlighting differences between hippocampal and cortical Aβ plaques. Glial fibrillary acidic protein-positive astrocytes showed a clear preference for clustering around NP in both the frontal cortex and hippocampus. These data support the notion that

Abbreviations: ACH, amyloid cascade hypothesis; AD, Alzheimer's disease; ADNC, Alzheimer's disease neuropathologic changes; APP, amyloid precursor protein; CRM, cytokines responsive microglia; DAM, disease associated microglia; DN, dystrophic neurites; ECM, extracellular matrix component; FOV, field of view; GFAP, glial fibrillary acidic protein; HLA, human leukocyte antigen; IHC, immunohistochemistry; IRM, interferon responsive microglia; MMSE, mini-mental state examination; MoCA, Montreal Cognitive Assessment; NFT, neurofibrillary tangles; non-NP, non-neuritic plaque; NP, neuritic plaques; PIG, plaque induced gene.

NP are intimately associated with the neuroimmune response in AD and underscore the importance of the interplay of protein deposits and the immune system in the pathophysiology of AD.

1 | INTRODUCTION

Alzheimer's disease (AD) is neuropathologically characterized by the presence of extracellular amyloid-β (Aβ) plaques, intracellular neurofibrillary tangles (NFT), and neurodegeneration (ATN) (Trejo-Lopez et al., 2022). The amyloid cascade hypothesis posits a linear cascade of events whereby aggregation of Aβ drives tau pathology, leading to neuronal loss and cognitive deficits (Hardy & Higgins, 1992; Hardy & Selkoe, 2002; Selkoe & Hardy, 2016). Recent studies tracking biomarker changes over 20 years from >1000 people confirmed that Aβ biomarkers change almost 18 years before clinical diagnosis, followed by tau biomarkers (10 years before diagnosis) and neurodegenerative changes measured by neurofilament light chain (9 years before diagnosis) (Jia et al., 2024; Li et al., 2024). These studies affirm the general concept of the amyloid cascade hypothesis. However, the amyloid cascade hypothesis, in its initial conception, strongly emphasized the contribution of neuronal cells in AD and failed to elucidate the role of glial cells such as microglia within the cascade of events leading to cognitive decline (Hardy & Higgins, 1992; Hardy & Selkoe, 2002). To provide a more holistic approach to AD pathogenesis, Bart De Strooper and Eric Karran proposed three sequential phases of AD. An initial biochemical phase of Aβ deposition and tau aggregation which leads to a cellular phase, whereby microglia, astrocytes, neurons, oligodendrocytes, and other cell types engage in compensatory feedback, which eventually wanes, leading to clinical phase manifesting with cognitive decline (De Strooper & Karran, 2016; Zeng et al., 2023). Other researchers proposed the amyloid cascade-inflammatory hypothesis, which suggests that microglial activation mediates the link between Aβ plaques and tau pathology (McGeer & McGeer, 2013), while others proposed that microglial dysfunction because of senescence drives AD pathogenesis (Lopes et al., 2008; Streit et al., 2009).

Despite the increasing number of studies on microglia, the role of these immune cells at the intersection of Aβ and tau pathology is still a matter of much debate (Bathe et al., 2024; Prokop et al., 2013; Prokop, Lee, et al., 2019; Tsering & Prokop, 2023). We have recently demonstrated that microglial activation and dystrophy follow the progression of AD neuropathologic changes (ADNC) (Prokop, Miller, et al., 2019; Tsering et al., 2023) and a recent review paper examining multiple microglial studies on postmortem human brain concluded that the number of microglia is similar between AD patients and healthy controls, but microglial phenotypes shift from homeostatic to phagocytic or dystrophic

in AD (Hopperton et al., 2018). The phenotypical and morphological shift of microglia is pronounced and exacerbated around Aβ plaques, suggesting that Aβ plaques are key triggers of local immune activation.

While there is some overlap, microglial responses to Aβ plaques are distinct between animal models and postmortem human brain tissues. First, a unique set of immune genes expressed around Aβ plaques termed disease-associated markers (DAM) in animal models (Keren-Shaul et al., 2017) only partially overlaps with microglia-associated gene expression in human (Del-Aguila et al., 2019; Mathys et al., 2019; Srinivasan et al., 2020). In a recent study, xenografted human microglia were shown to adopt antigen-presenting response (HLA), interferon response (IRM), and cytokines response (CRM) besides the DAM signature (Mancuso et al., 2024), supporting the notion that microglia-associated gene expression differs between animal models and the human disease condition. Second, in animal models of amyloidosis, microglial activation is usually observed uniformly around all Aβ plaques, since most animal models predominantly exhibit one morphological type of Aβ plaques, rather than the full spectrum of morphological subtypes seen in postmortem human brains (Xu et al., 2020). For example, the CRND8 mouse model of amyloidosis mainly shows dense-cored plaques (Yuan et al., 2013), while human postmortem brain tissue exhibits many different morphological subtypes of Aβ plaque such as diffuse plaques, dense-cored plaques, cotton-wool plaques (Crook et al., 1998), coarse-grained plaques (Boon et al., 2020), and neuritic plaques (NP) (reviewed in Tsering & Prokop, 2023).

Interestingly, not all morphological subtypes of Aβ plaques elicit a strong local immune activation in the postmortem human brain. Dense-cored plaques are shown to exhibit more microgliosis compared to diffuse plaques (Ohgami et al., 1991). However, the microglial response around other morphological subtypes of Aβ plaques is not well characterized. One subtype of Aβ plaques called neuritic plaque, characterized by swollen dystrophic axons, deserves special consideration for being specific to AD and being nexus of Aβ and tau pathology (Tsering & Prokop, 2023).

We have recently shown that non-NP (non-NP) are transformed into NP during the progression of ADNC (classification of ADNC based on Thal phase of Aβ plaque pathology, Braak NFT stage, and Consortium to establish a registry for Alzheimer's disease [CERAD] neuritic plaque score) and likely drive cortical, but not hippocampal, spread of NFT (Tsering et al., 2023). Based on this finding, we hypothesize that neuritic dystrophy around Aβ plaques induces

microglia clustering and phenotypic shift in a brain region-specific manner. We therefore examined microglial clustering and phenotype as well as astrocytic clustering around NP and non-NP during the progression of ADNC. We show that Iba1-positive microglia preferentially cluster around NP and CD68-positive phagocytic microglia show a strong preference to cluster around NP in both hippocampus and frontal cortex. A similar preferential clustering is observed for CD11c and ferritin-positive microglia in the frontal cortex, while this preference is less pronounced in the hippocampus, indicating potential differences between hippocampal and cortical Aβ plaques. Additionally, glial fibrillary acidic protein (GFAP)-positive astrocytes showed a clear preference for clustering around NP in both frontal cortex, and hippocampus.

2 | METHODS

2.1 | Patient samples

Postmortem brain tissues were selected from the University of Florida Human Brain and Tissue Bank (UF HBTB) with approval from the University of Florida Institutional Review Board (IRB201600067). All the patients or their next-of-kin gave informed consent for the brain donation. Case details are provided in Table 1 and Table S1. Montreal Cognitive Assessment (MoCA) scores are converted to the Mini-Mental State Examination (MMSE) based on conversion table (Fasnacht et al., 2023). Cases were grouped into different ADNC—"low AD" ($n = 10$), "Intermediate AD" ($n = 10$), and "high AD" ($n = 20$) based on the NIA-AA guideline for pathological diagnosis which constitutes the Thal phase of Aβ plaques (A), Braak and Braak NFT stage (B), and CERAD neuritic plaque score (C)—"ABC" score (Montine et al., 2012). "High AD" cases were further grouped into "pure" ($n = 10$) Aβ and tau pathology and cases with additional Lewy body pathology "high AD mixed pathology" ($n = 10$). Brain sections were taken from medial pre-frontal cortex and hippocampus.

2.2 | Gallyas Silver impregnation and double IHC staining

Modified Gallyas Silver staining protocol was combined with the double immunohistochemistry staining method to visualize microglial clustering around non-NP and NP. Postmortem brain tissue sections with 8 μm thickness were deparaffinized twice in xylene for 5 min each and then in ethanol series (100%, 100%, 90%, 70%) for 1 min each. After a brief rinse in dH$_2$O, sections were placed in 5% period acids for 5 min using a glass Coplin jar. Sections were washed twice for 5 min in dH$_2$O and then placed in alkaline silver iodide solution for 1 min. Rinsed a few times with dH$_2$O and washed in 0.5% acetic acid for 10 min, followed by developing in developer solutions (developer solutions were stored in a refrigerator at 4°C for 30 min before developing) for 17–25 min. Following a 3-min wash in 0.5% acetic acid and a 5-min wash in dH$_2$O, sections were placed

in 0.1% gold chloride for 5 min. After a brief rinse in dH$_2$O, sections were placed in 1% sodium thiosulfate solution for 5 min and then washed in tap water before starting the IHC portion. For the IHC part, sections were incubated in a solution of 0.1 M Tris (pH 7.6) and 0.05% Tween using a pressure cooker for 15 min to retrieve the antigen. Next, sections were immersed in freshly prepared PBS/H$_2$O$_2$ solution with 10% Triton-X for 20 min to quench endogenous peroxidases, followed by multiple washes with tap water and a 5-min wash in 0.1 M Tris (pH 7.6). Sections were then incubated in 2.5% Normal Horse Serum for 20 min, followed by blocking in 2% FBS/0.1 M Tris (pH 7.6) for at least 5 min. Primary antibodies raised from different species were diluted in a blocking buffer and applied to the sections for overnight incubation. Antibody details are in Additional file 2: Table S2. The following day, antibodies were gently washed away from the sections by 0.1 M Tris (pH 7.6) and then sections were blocked in 2% FBS/0.1 M Tris (pH 7.6) for at least 5 min. Then, biotinylated secondary antibody (Anti-Rabbit or Mouse ImmPRESS-HRP Polymer Reagent, Vector Labs) was applied on the sections and incubated for 30 min in a humidified chamber at room temperature, followed by brief wash with 0.1 M Tris (pH 7.6) and then 1- to 2-min development with 3,3′-diaminobenzidine (Vector DAB, Vector Labs, catalog #51275). Next, sections were washed in tap water for 10 min and then incubated with alkalinated secondary antibody (ImmPRESS-AP [Alkaline Phosphatase] Polymer anti-Mouse Reagent, Vector Labs, catalog# MP-5402) for 1 h. After that, sections were developed by using an Alkaline Phosphatase substrate kit (Vector Red Substrate Kit, AP- SK-5100) for 5 min, and then counterstained with hematoxylin (Sigma Aldrich, catalog# 51275) for 1 min. Finally, sections were rinsed in tap water and washed twice in isopropanol for 5 min each before coverslipping with VectaMount Express mounting medium (Vector Laboratories catalog# ZK0209).

2.3 | Immunofluorescence

For immunofluorescence, 8-μm thick sections were deparaffinized with xylene and rehydrated with descending ethanol series as described in the IHC method section above. Sections were immersed in 0.25% KMnO$_4$ for 5 min, followed by a crude wash with water, and then immersed in 1% K$_2$S$_2$O$_5$/1% oxalic acid for 5 min. After that, sections were immersed in 0.02% Thioflavin-S for 8 min, followed by a brief wash in water and then in 70% ethanol for 1 min. Sections were treated with citrate for antigen retrieval using the pressure cooker. After washing three times with 0.1 M Tris (pH 7.6) and blocking with 2% FBS/0.1 M Tris (pH 7.6) for at least 5 min, sections were incubated with primary antibodies in the blocking solution for overnight. Pan-microglia marker, IBA1 (Abcam, catalog ab178847), and p-tau antibody, 7F2 (Giasson Lab) were used. The next day, sections were washed with 0.1 M Tris (pH 7.6) and then incubated with secondary antibodies (Invitrogen Alexa Fluor 647 goat anti-mouse IgG and Invitrogen Cy3 goat anti-rabbit IgG) at room temperature for 1 h. Sections were washed and mounted with fluorescent mounting media containing DAPI.

TABLE 1 Neuropathology data for cases used in this study.

Sample	Neuropath	Thal	Braak	CERAD	APOE	Sex	Age	PMI	MMSE score	Alpha synuclein	LATE-NC
1	Low AD	2	II	None	3/4	F	63	168	NA	No	No
2	Low AD	1	I	None	3/3	F	65	15	NA	No	No
3	Low AD	1	I	None	2/3	M	68	48	NA	No	No
4	Low AD	1	IV	None	2/3	F	74	7.5	NA	No	No
5	Low AD	1	III	None	3/4	F	79	72	NA	No	No
6	Low AD	3	II	Sparse	3/3	M	79	34	NA	No	No
7	Low AD	3	II	Sparse	3/3	M	81	144	NA	No	No
8	Low AD	1	II	None	3/3	M	90	14	NA	No	No
9	Low AD	3	II	Mild	3/3	M	91	72	NA	No	No
10	Low AD	3	II	Sparse	3/3	F	96	16	NA	No	No
11	Intermediate AD	5	IV	Frequent	3/3	M	72	72	NA	No	No
12	Intermediate AD	3	IV	Moderate	3/4	F	74	192	NA	No	No
13	Intermediate AD	5	III	Sparse	2/4	M	78	4	18/30*	No	No
14	Intermediate AD	4	III	Moderate	3/3	F	83	192	NA	No	No
15	Intermediate AD	5	IV	Moderate	3/3	M	86	48	NA	No	No
16	Intermediate AD	4	III	Sparse	3/4	M	86	12	NA	No	No
17	Intermediate AD	4	IV	Frequent	3/3	F	89	8	24/30	No	No
18	Intermediate AD	5	IV	Frequent	3/4	M	90	7	NA	No	No
19	Intermediate AD	4	V	Moderate	3/4	F	99	8	NA	No	No
20	Intermediate AD	5	IV	Frequent	3/3	F	100	18	NA	No	No
21	High AD Pure	5	VI	Frequent	3/3	F	63	10	NA	No	No
22	High AD Pure	5	VI	Frequent	3/4	M	63	2	NA	No	No
23	High AD Pure	5	VI	Frequent	3/3	M	66	5	NA	No	No
24	High AD Pure	5	V	Frequent	3/3	F	78	5	NA	No	No
25	High AD Pure	5	V	Frequent	3/4	M	78	20	15/30	No	No
26	High AD Pure	4	V	Frequent	3/4	M	84	16	9/30	No	No
27	High AD Pure	4	V	Frequent	3/4	F	85	18	23/30	No	No
28	High AD Pure	5	V	Frequent	3/4	F	86	14	13/30	No	No
29	High AD Pure	5	V	Frequent	3/3	M	95	5	NA	No	No
30	High AD Pure	5	V	Frequent	2/4	F	97	10	NA	No	No
31	High AD mixed	5	V	Frequent	3/3	F	63	12	26/30	Yes	Stage 3
32	High AD mixed	5	VI	Frequent	3/3	M	70	4	13/30	Yes	Stage 2
33	High AD mixed	5	VI	Frequent	4/4	F	75	8	22/30	Yes	Stage 1
34	High AD mixed	5	VI	Frequent	4/4	F	76	3	14/30	Yes	Stage 3
35	High AD mixed	5	V	Frequent	3/3	F	78	12	NA	Yes	Stage 2
36	High AD mixed	5	VI	Frequent	3/4	M	78	22	NA	Yes	No
37	High AD mixed	5	V	Frequent	3/4	M	80	21	NA	Yes	Stage 2
38	High AD mixed	5	V	Frequent	3/4	F	83	6	NA	Yes	No
39	High AD mixed	5	V	Frequent	3/3	M	85	25	NA	Yes	No
40	High AD mixed	5	VI	Frequent	4/4	M	91	14.25	NA	Yes	Stage 1

Abbreviations: AD, Alzheimer's disease; APOE, Apolipoprotein E; CERAD, Consortium to establish a registry for Alzheimer's disease; LATE-NC, limbic-predominant age-related TDP-43 encephalopathy neuropathologic change; MMSE, mini-mental state examination; PMI, postmortem interval.

*MOCA score was converted into MMSE score.

2.4 | Data analysis

All the immunohistochemistry-stained brain slides were scanned at 40× magnification using an Aperio AT2 slide scanner (Leica Biosystems). Scanned slides were analyzed using open-source digital pathology software, QuPath (Version 0.4.3) (Bankhead et al., 2017). For each brain region from the individual case, 5 equally and randomly distributed rectangles (area $\mu m^2 = 1\,125\,154$, perimeter

μm = 4500) were annotated on the digital slide and then manually counted the number of CD68+/Ferritin+/Cd11c+/GFAP+ clusters around non-NP and NP by blinded observers (Figure S1). Each data point represents percentage of non-NP or NP that are positive for each glial markers from individual sample. Error bars on graphs represent the standard deviation (SD) of the mean. Clustering is defined as two or more cells touching individual Aβ plaque.

Immunofluorescence images were captured by confocal microscopy (Nikon CSY-W1 SoRA) at 20× magnification using the same exposure and contrast for each channel. Five fields of view (FOV) for each sample were captured. Image J-Fiji software was used for immunofluorescence analysis (Schindelin et al., 2012). For quantification, the percent average of IBA1+ non-NP or NP from 5 FOVs was quantified from each sample. Each data point represents percentage of IBA1+ non-NP or IBA1+ NP from individual sample.

2.5 | Statistics

All the immunohistochemistry quantification analyses were done using GraphPad Prism (Version 10.2.3). For analysis with 2 study groups, Shapiro–Wilk test was run to test the normality of data. Wilcoxon matched-pairs signed rank test (two-tailed) was used to compare the percent differences in microglial or astrocytic clustering between non-NP and NP. For analysis with more than 2 study groups, Kruskal–Wallis test with Dunn's multiple comparisons test was used. No test for outliers was conducted to exclude any data points. Full statistical reports for each figure are in the Table S3. Sample size calculation was not performed; we used 10 samples per group based on our initial observation of a large effect size between non-NP and NP in glial clustering. Additionally, similar studies have used comparable sample sizes to obtain meaningful results (Paasila et al., 2019, 2020).

3 | RESULTS

3.1 | Microglia preferentially cluster around NP

To examine the microglia response around non-NP and NP, we stained 10 frontal cortex samples (Interm AD = 5, high AD = 5) from patients with intermediate and high Alzheimer's disease neuropathological changes (ADNC) for Iba1 (microglia), 7F2 (dystrophic neurites [DN]) (Xia et al., 2020) and Thioflavin-S (amyloid plaques) and quantified clustering of microglia around NP, and non-NP. NP were defined as Thioflavin-positive deposits with 7F2-positive DN and non-NP were characterized by positivity for Thioflavin and absence of 7F2-positive DN. Microglial clustering, defined by the presence of two or more cells around non-NP and NP was manually quantified by blinded observers. This analysis revealed that 93% of NP show clustering of IBA1+ microglia around them, compared to only 27% of non-NP (Figure 1) suggesting preferential clustering of microglia around p-tau+ NP.

3.2 | Phagocytic (CD68-positive) microglia show preferential clustering around NP in frontal cortex and hippocampal regions

To further characterize microglial clustering around Aβ plaques, we utilized CD68, a marker for phagocytic microglia (Hendrickx et al., 2017), and stained 40 postmortem brain samples (10 samples with low ADNC, 10 samples with intermediate ADNC, and 20 samples with high ADNC) from a previously published cohort (Tsering et al., 2023) to quantify microglia clustering around NP and non-NP. We combined high AD "pure" (only Aβ and tau pathology) cases with high AD "mixed" cases (Aβ, tau, and alpha synuclein co-pathology), since we observed no significant differences in glial clustering between the high AD "pure" and high AD "mixed" groups (Figure S4). For each case, we analyzed frontal cortex and hippocampus separately, since we previously demonstrated that NP drive NFT pathology in cortical regions, but not in the hippocampus (Tsering et al., 2023), hinting at brain-region specific differences in the interplay between NP and NFT. We combined immunohistochemistry for CD68 and Aβ with Gallyas Silver staining to examine microglial clustering around non-NP and NP. Here, NP are defined by positivity for Aβ (anti-Aβ antibody, D12B2) and the presence of Gallyas Silver positive DN, while non-NP are defined by only Aβ and the absence of Gallyas Silver positive DN. CD68+ microglia are significantly more clustered around NP in Intermediate AD and high AD cases compared to non-NP (Figure 2) in both the frontal cortex and hippocampus. In low AD cases, CD68+ microglia tend to cluster more around NP, but statistical significance is not reached because of low number of NP in low AD cases.

3.3 | DAM microglia (CD11c-positive) and dystrophic microglia (ferritin-positive) preferentially cluster around NP with brain region-specific differences

Next, we investigated the clustering of CD11c-positive cells around non-NP and NP. CD11c is associated with microglial activation and is considered part of the DAM signature (Keren-Shaul et al., 2017; Wlodarczyk et al., 2017). Using a triple stain of Gallyas silver staining and immunohistochemistry for Aβ (D12B2) and CD11c and the same definition of NP and non-NP as described above, we found that CD11c+ microglia are significantly more clustered around NP compared to non-NP in Intermediate AD cases and high AD cases (Figure 3) in frontal cortex and hippocampus, while there were no differences in clustering of CD11c-positive cells in low AD cases (Figure 3). Although the differences in microglia clustering between non-NP and NP were statistically significant in both frontal cortex and hippocampus, we noted a substantial amount of CD11c-positive microglia clustering around non-NP in the hippocampus (Figure 3).

A similar picture was seen when we examined the clustering of ferritin-positive dystrophic microglia (Lopes et al., 2008) around
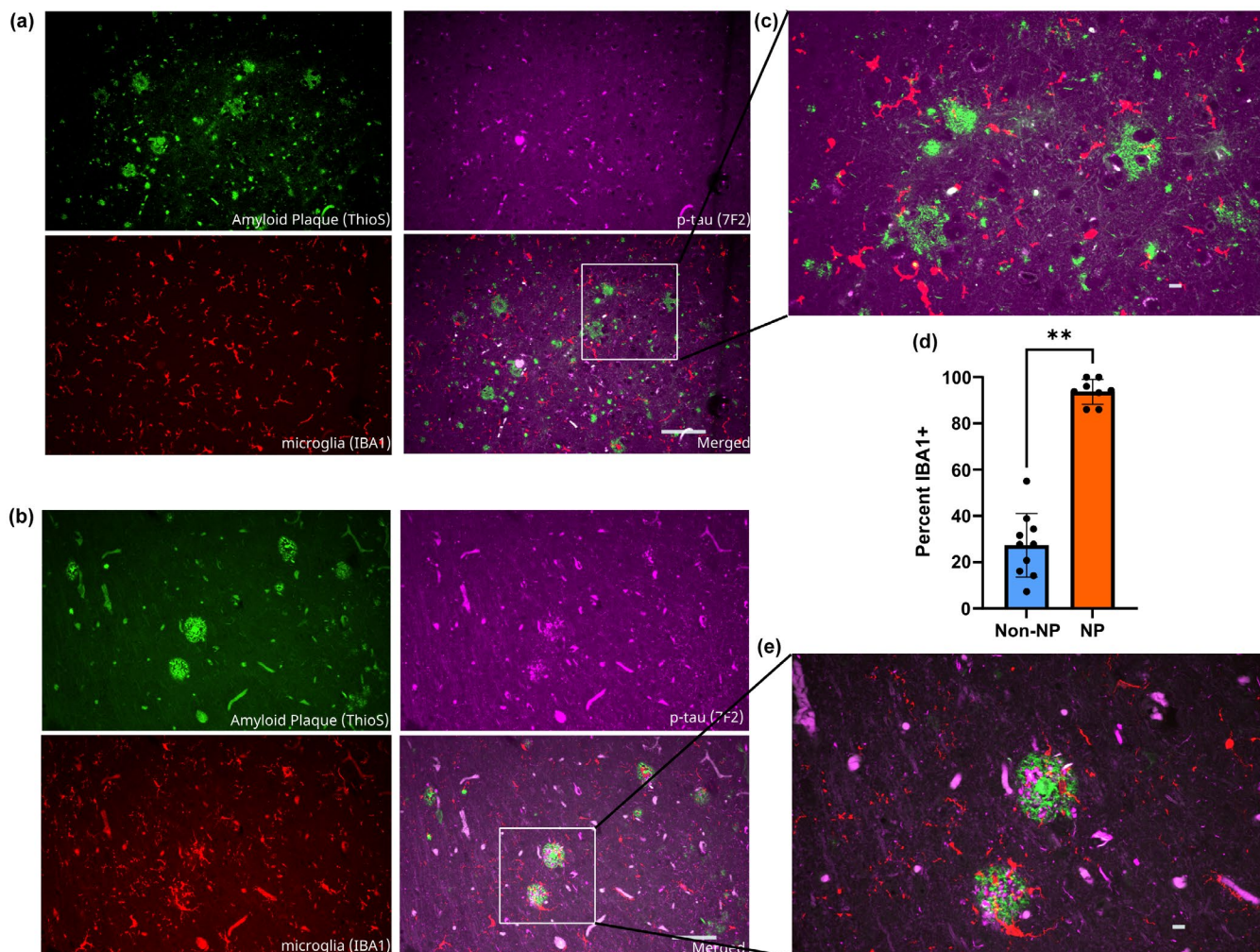
FIGURE 1 IBA1+ microglia cluster around p-tau+ neuritic plaques. Frontal Cortex staining of (a) non-neuritic plaque and (b) p-tau+ neuritic plaque using pan-microglia marker, Iba1 (red), amyloid plaque dye, Thioflavin-S (green) and p-tau antibody, 7F2 (magenta). Scale bar = 100 μm. Higher magnification (40×) image of (c) non-neuritic plaque and (e) neuritic plaque with microglial clustering. Scale bar = 10 μm. (d) Quantification of the percent Iba1+ microglial clustering around non-neuritic plaques (non-NP) and NP. Data are presented as mean with SD. Shapiro–Wilk test was run to test the normality of data. Wilcoxon matched-pairs signed rank test (two-tailed) was used to compare the percent differences in IBA1+ microglial clustering between non-NP and NP. $N = 10$ human postmortem samples (5 intermediate Alzheimer's disease [AD] cases, 5 high AD cases). $**p < 0.01$.

non-NP and NP, using a triple stain of Gallyas silver staining and immunohistochemistry for Aβ (D12B2) and Ferritin. Ferritin+ microglia show significantly more clustering around NP compared to non-NP in both frontal cortex and hippocampus in intermediate and high AD cases (Figure 4), while also here a substantial portion of non-NP showed clustering of ferritin-positive microglia in the hippocampus (Figure 4).

In addition to qualitative differences in clustering of microglia between different brain regions, we also observed brain region-specific differences in the number of microglia positive for a specific marker per NP. In the hippocampus, the number of CD68/CD11c/Ferritin+ microglia per NP is significantly higher compared to frontal cortex in high AD cases (Figure S6). Furthermore, when assessing clustering of CD68+/CD11c+/Ferritin+/GFAP+ cell around Aβ plaque irrespective of plaque subtype, we observed significant increases or trends toward increased microglial clustering around Aβ

plaques during the progression of ADNC in the frontal cortex, while this trend is not observed in the hippocampus for all examined glial markers except for CD68 (Figure S5).

3.4 | Astrocytes also show preferential clustering around NP

Astrocytes play an important role in regulating central nervous system homeostasis, vasculature, and synapses (Khakh & Sofroniew, 2015; Sofroniew & Vinters, 2009). Astrocytes respond and react to foreign insults and pathological conditions such as AD, resulting in reactive astrogliosis (Matias et al., 2019). GFAP is a type III intermediate filament, an important cytoskeleton component that is expressed by astrocytes and is widely used as a marker of reactive astrocytes. Using a triple stain of Gallyas silver staining and immunohistochemistry for
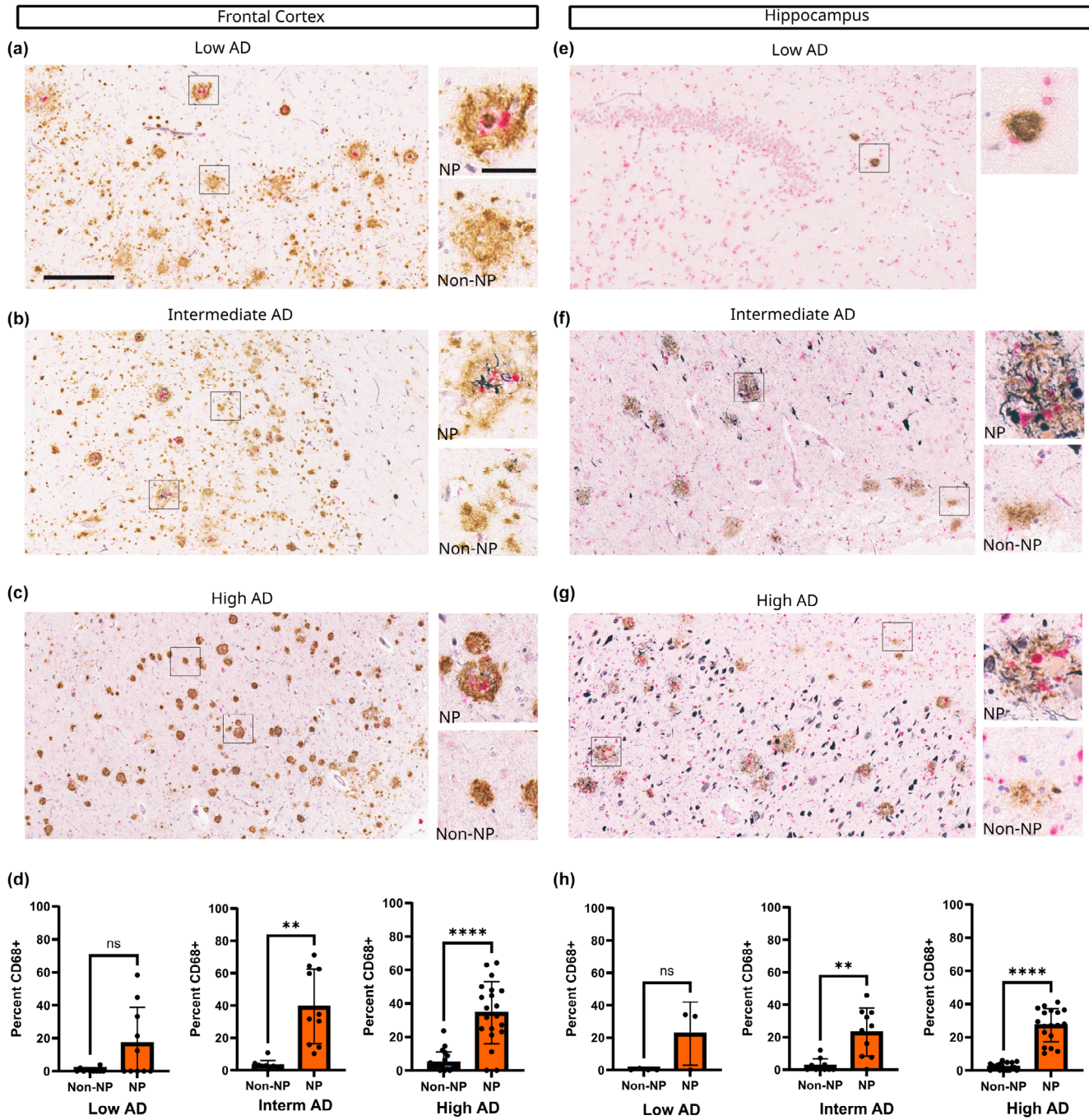
FIGURE 2 CD68+ microglia are significantly more clustered in and around neuritic plaques (NP). Frontal cortex (a–d). Frontal cortex images from low Alzheimer's disease (AD) (a), intermediate AD (b), and high AD (c) were shown in low magnification (300 μm) with higher magnification (60 μm) images of CD68+ NP and CD68− non-NP on the side. NP and non-NP are defined by the presence of Gallyas Silver staining+ dystrophic neurite (black) around anti-amyloid-β antibody D12B2 (brown). CD68+ microglial clustering is defined by the presence of CD68+ cells (Pink) around non-NP and NP. (d) Quantification of CD68+ microglial clustering around non-NP and NP in frontal cortex from different ADNC– low AD ($n = 10$ cases), intermediate AD ($n = 10$ cases), and high AD ($n = 20$ cases). CD68+ microglial clustering is significantly higher in NP compared to non-NP in intermediate AD (p-value = 0.0020) and high AD (p-value < 0.0001). Hippocampus (e–h). Hippocampus images from low AD (e), intermediate AD (f), and high AD (g) were shown in low magnification (300 μm) with higher magnification (60 μm) images of CD68+ NP and CD68− non-NP on the side. (h) Quantification of CD68+ microglial clustering around non-NP and NP in hippocampal regions from low AD cases ($n = 4$ cases), intermediate AD ($n = 10$ cases, and low AD cases ($n = 4$ cases). CD68+ microglial clustering is significantly higher around NP in intermediate AD (p-value = 0.0039) and high AD cases (p-value < 0.0.001). In low AD cases (p-value = 0.5), there are no significant differences but the trend toward higher clustering around NP. Data are presented as mean with SD. Shapiro–Wilk test was run to test the normality of data. Wilcoxon matched-pairs signed rank test (two-tailed) was used to compare the percent differences in IBA1+ microglial clustering between non-NP and NP. **p < 0.01, ****p < 0.0001.
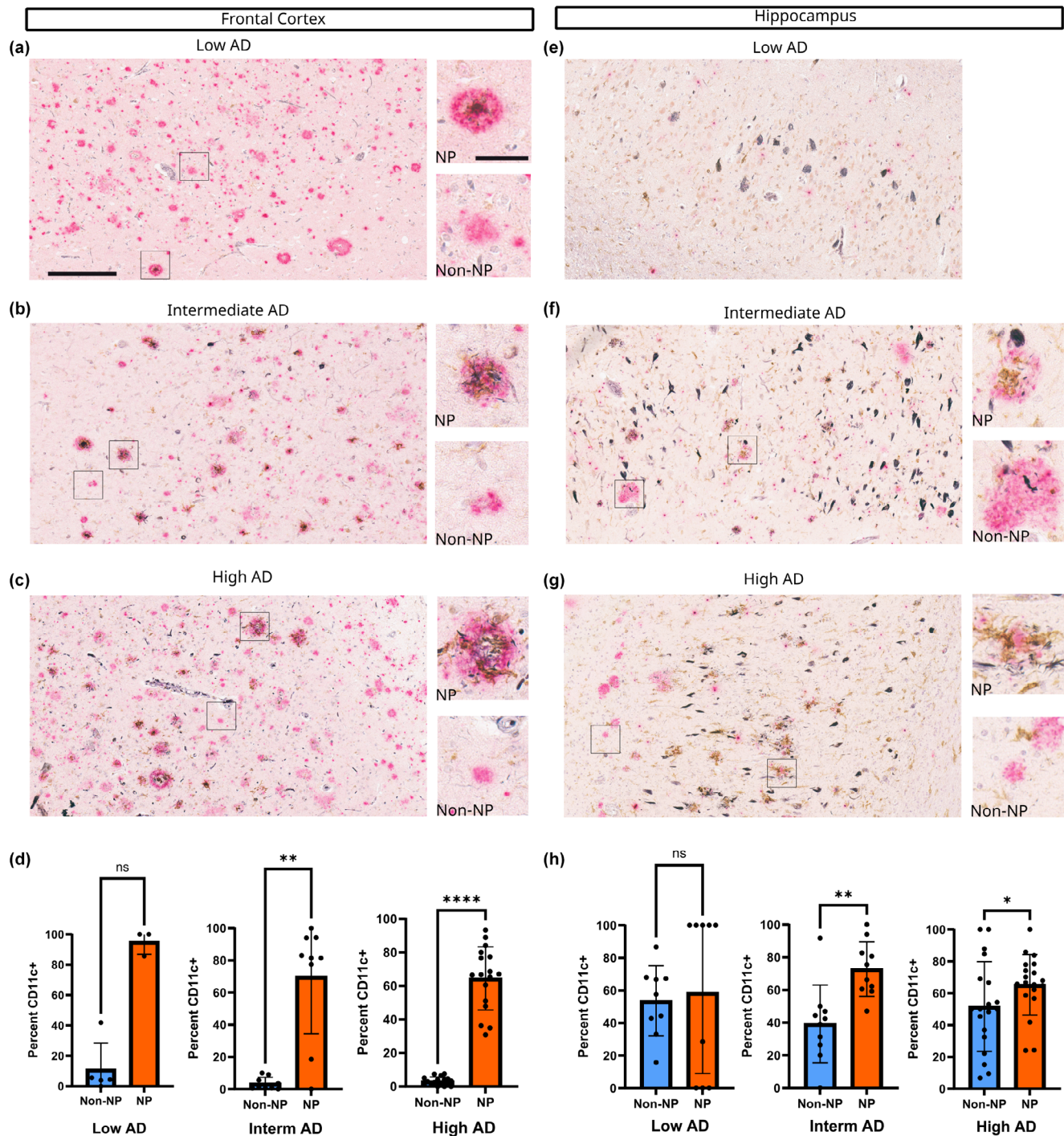
FIGURE 3 Disease-associated (DAM) microglia marker CD11c+ are significantly more clustered in and around neuritic plaques (NP). Frontal cortex (a–d). Frontal cortex images from (a) low Alzheimer's disease (AD), (b) intermediate AD, and (c) high AD were shown in low magnification (300μm) with higher magnification (60μm) images of CD11c+ NP and CD11c− non-NP on the side. NP and non-NP are defined by the presence of Gallyas Silver staining+ dystrophic neurite (black) around anti-amyloid-β antibody Ab5 (Pink). CD11c+ microglial clustering is defined by the presence of CD11c+ cells (brown) around non-NP and NP. (d) Quantification of CD11c+ microglial clustering around non-NP and NP in frontal cortex from different ADNC− low AD ($n = 5$ cases), intermediate AD ($n = 9$ cases), and high AD ($n = 17$ cases). CD11c+ microglial clustering is significantly higher in NP compared to non-NP in intermediate AD (p-value = 0.0078) and high AD cases (p-value < 0.0001). In low AD cases (p-value = 0.2500), there are no significant differences. Hippocampus (e–h). Hippocampus images from (e) low AD, (f) intermediate AD, and (g) high AD were shown in low magnification (300μm) with higher magnification (60μm) images of CD11c+ NP and CD11c− non-NP on the side. (h) Quantification of CD11c+ microglial clustering around non-NP and NP in hippocampus from low AD cases ($n = 9$ cases), intermediate AD cases ($n = 10$ cases), and high AD cases ($n = 19$ cases). CD11c+microglial clustering is significantly higher around NP in intermediate AD (p-value = 0.0039) and high AD (p-value = 0.0181). In low AD cases (p-value = 0.8203), there are no significant differences. Data are presented as mean with SD. Shapiro–Wilk test was run to test the normality of data. Wilcoxon matched-pairs signed rank test (two-tailed) was used to compare the percent differences in IBA1+ microglial clustering between non-NP and NP. *$p < 0.05$, **$p < 0.01$, ****$p < 0.0001$.
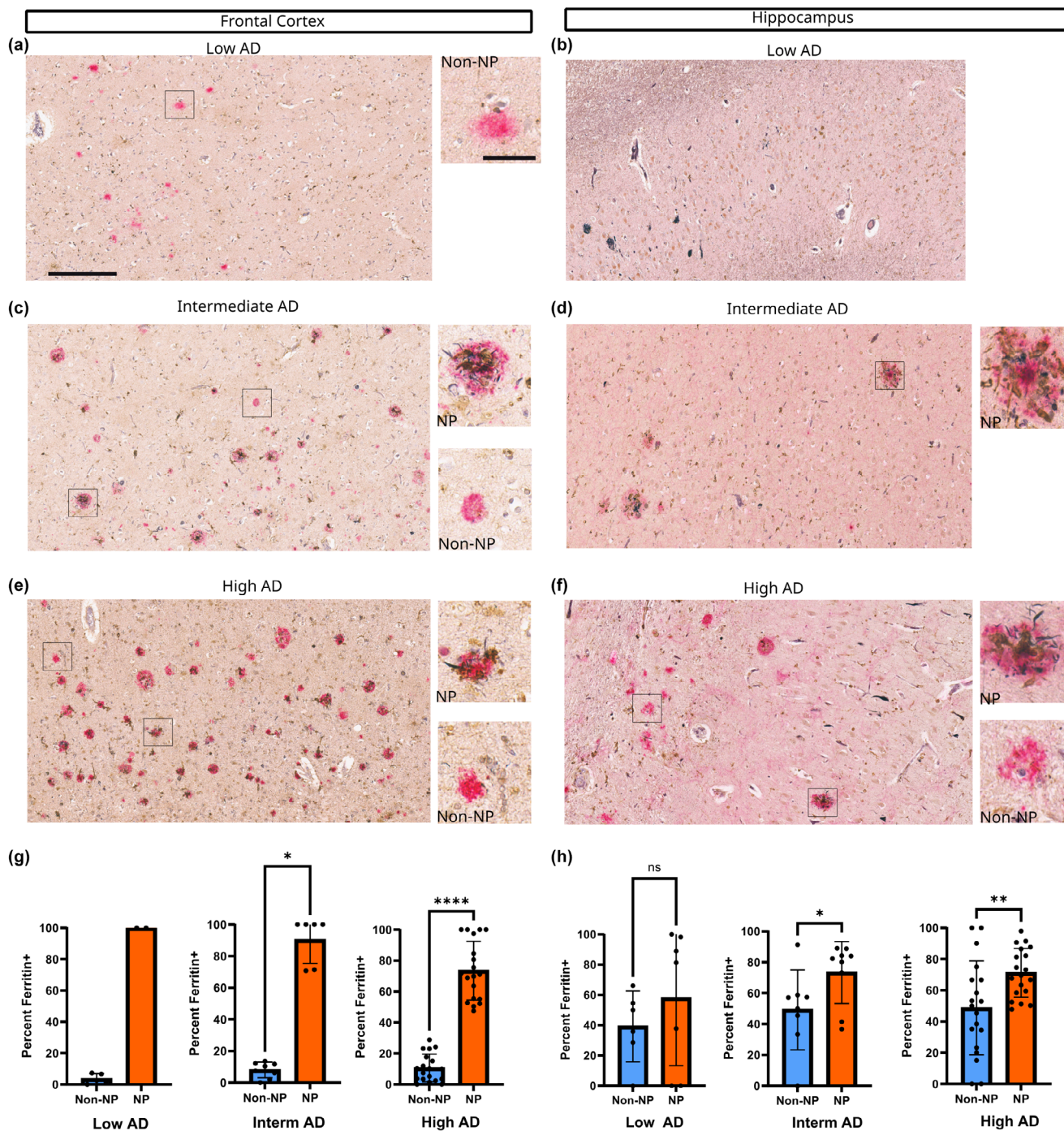
FIGURE 4 Dystrophic microglia marker, Ferritin are significantly more clustered in and around neuritic plaques (NP). Frontal cortex (a–d). Frontal cortex images from (a) low Alzheimer's disease (AD), (b) intermediate AD, and (c) high AD were shown in low magnification (300 μm) with higher magnification (60 μm) images of Ferritin+ NP and Ferritin− non-NP on the side. NP and non-NP are defined by the presence of Gallyas Silver staining+ dystrophic neurite (black) around anti-amyloid-β antibody Ab5 (pink). Ferritin+ microglial clustering is defined by the presence of Ferritin+ cells (brown) around non-NP and NP. (d) Quantification of Ferritin+ microglial clustering around non-NP and NP in frontal cortex from different ADNC− low AD ($n=5$ cases), intermediate AD ($n=8$ cases), and high AD ($n=19$ cases). Ferritin+ microglial clustering is significantly higher in NP compared to non-NP in intermediate AD cases (p-value$=0.0312$) and high AD cases (p-value<0.0001). Hippocampus (e–h). Hippocampus images from (e) low AD, (f) intermediate AD, and (g) high AD were shown in low magnification (300 μm) with higher magnification (60 μm) images of Ferritin+ NP and Ferritin− non-NP on the side. (h) Quantification of Ferritin+ microglial clustering around non-NP and NP in hippocampal regions from low AD cases ($n=7$ cases), intermediate AD cases ($n=9$ cases), and high AD cases (n=19 cases). Ferritin+ microglial clustering is significantly higher around NP in intermediate AD (p-value$=0.0391$) and high AD (p-value$=0.0017$). In low AD cases, there are no significant differences. Data are presented as mean with SD. Shapiro–Wilk test was run to test the normality of data. Wilcoxon matched-pairs signed rank test was (two-tailed) used to compare the percent differences in IBA1+ microglial clustering between non-NP and NP. $*p<0.05$, $**p<0.01$, $****p<0.0001$.

Aβ (D12B2) and Ferritin, we analyzed astrocytic clustering around NP and non-NP. Here we found that GFAP-positive astrocytes are preferentially clustered around NP compared to non-NP in both frontal cortex and hippocampus (Figure 5).

Assessing the spatial distribution and pattern of microglial and astrocytic clustering around NP, we observed that microglia tend to cluster within or around the inner layer of NP and astrocytes tend to cluster outside of NP or around the outer layer of NP.

4 | DISCUSSION

In this study, we examined the clustering of microglia and astrocytes around non-NP and NP during the progression of ADNC in the frontal cortex and hippocampus using different phenotypic markers. In the frontal cortex, we observed that microglia of different activation states (Iba1, Ferritin, CD68, and CD11c positive) and astrocytes (GFAP-positive) preferentially clustered in and around NP compared to non-NP. In the hippocampus, a similar clustering of microglia and astrocytes around NP is observed but substantial clustering of CD11c or Ferritin- positive microglia is also observed around non-NP suggesting that the evolution of Aβ plaque subtypes may be different in the frontal cortex and hippocampus. In general, glial clustering around Aβ plaques increased with progression of ADNC, but we did not observe sex and Apolipoprotein E genotype differences in CD68+/CD11c+/Ferritin+/GFAP+ clustering around non-NP and NP in frontal cortex and hippocampus (Figures S2 and S3).

Previous studies have examined the effect of local immune activation around Aβ plaques. However, these studies examined the differences in microgliosis or astrogliosis between diffuse plaques and dense-cored plaques using dye such as thioflavin or Congored in a limited number of cases (Serrano-Pozo et al., 2013). In this study, we classified the Aβ plaques into non-NP and NP defined by the presence of Gallyas silver staining+ dystrophic neurites around Aβ plaques (Ab5 or D12B2 immunohistochemistry). Both diffuse plaques and dense-cored plaques can be either non-neuritic or neuritic. A previous study showed that 80% of dense-cored plaques have neuritic dystrophy while only 20% of diffuse plaque have neuritic dystrophy (Dickson & Vickers, 2001). Although diffuse plaques often overlap with non-neuritic and dense-cored plaque frequently overlap with NP, not all diffuse plaques are non-neuritic and not all dense-cored plaques are NP. This distinction is important to understand as to whether the microglial clustering around Aβ plaques is driven by toxic Aβ species or neuritic dystrophy. Our data show that microglial clustering is significantly more pronounced around NP compared to non-NP, which may suggest that damaged dystrophic neurites around Aβ plaques may be a trigger to recruit microglia to the Aβ plaque (Jury-Garfe et al., 2024) (Figure 6a). However, the cross-sectional nature of our study makes it difficult to answer whether glial clustering around NP is the consequence of Aβ toxicity or neuritic dystrophy. We also observed clustering of CD68 and CD11c in and around dense-core plaques without neuritic dystrophy in all stages of ADNC progression, suggesting that some

non-NP plaques are also driving glial clustering. It is conceivable Aβ deposits at some point become neurotoxic and therefore drive NP formation as well as glial clustering. Recent studies show that many proteins co-accumulate with Aβ in plaques (Bai et al., 2020; Johnson et al., 2022; Levites et al., 2024), and these amyloidosis-associated proteins could be responsible for driving neurotoxicity and recruiting a glial response.

An alternative explanation is that microglia-driven inflammation is intimately involved in the process of neurotoxicity and formation of dystrophic neurites. Ablation of microglia using colony-stimulating factor 1 receptor (CSF1R) inhibitors in animal models of Aβ amyloidosis led to increased neuritic dystrophy around Aβ plaques (Delizannis et al., 2021; Sosna et al., 2018; Spangenberg et al., 2019). Loss of the microglia receptor TREM2 and presence of genetic TREM2 variants associated with an increased risk of developing AD were associated with reduced microglia clustering, increased neuritic dystrophy, and overall tau burden in animal models as well as human postmortem tissue (Leyns et al., 2019; Prokop, Miller, et al., 2019; Wang et al., 2016; Yuan et al., 2016). These studies suggest that microglia are responsible for the formation of a physical barrier around Aβ plaques, leading to compaction of the Aβ deposit to reduce neuritic damage. Microglia clustering around dense-core plaques without neuritic dystrophy, which we observed in our cohort as well as shown by others (Paasila et al., 2020), may support the notion that microglia clustering precedes neuritic dystrophy during the progression of ADNC (Figure 6b). Alternatively, preferred microglia clustering around NP compared to non-NP in Intermediate AD and high AD cases may be indicative of a microglia response to neuronal injury in the form of DN formation. To further complicate the picture, the presence of ferritin-positive microglia around NP may indicate that microglia are undergoing cellular senescence (Lopes et al., 2008; Streit et al., 2009, 2021) when clustered around NP. A recent study showed that autophagy deficiency promotes senescence and suppresses disease-associated microglia (Choi et al., 2023). It is tempting to speculate that microglia are successful in phagocytosis of Aβ in early disease stages. However, when the Aβ burden reaches a certain threshold, microglia cluster around Aβ plaques to form a barrier and eventually fail in their protective function because of exhaustion or autophagy deficiency, resulting in exacerbation of neuritic dystrophy, which acts as a favorable environment for tau seeding (Gratuze et al., 2021; Leyns et al., 2019; Shahidehpour et al., 2012) (Figure 6c).

We also observed that astrocytes preferentially clustered around NP, albeit more distant than microglia, forming an outer layer of reactive cells around Aβ plaques. It has been shown that microglial activation incites or drives astrocytic reactivity (Liddelow et al., 2017). When activated, astrocytes release inhibitory extracellular matrix components (ECM) around neuronal damage sites to restrict further damage to the surrounding tissue (Busch & Silver, 2007; Dewitt & Silver, 1996; Fitch & Silver, 2008). It is conceivable that inhibitory ECM molecules attenuate the microglial response, leading to more neuritic dystrophy.

While microglia clustering is strongly biased toward NP in the frontal cortex, we noted substantial microglia clustering around
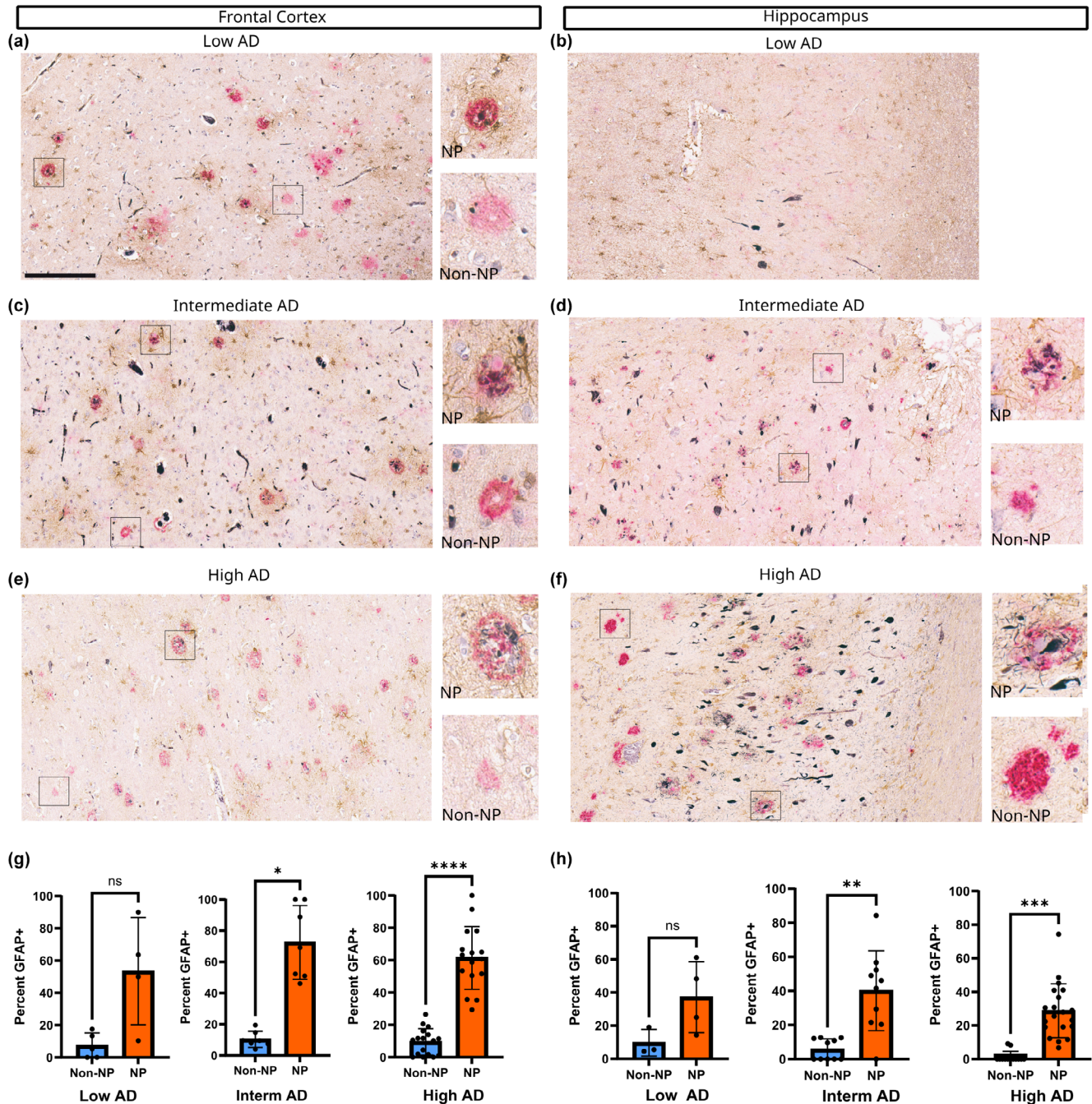
FIGURE 5 Reactive astrogliosis marker, glial fibrillary acidic protein (GFAP) is significantly more clustered around neuritic plaques (NP). Frontal cortex (a–d). Frontal cortex images from (a) low Alzheimer's disease (AD), (b) intermediate AD, and (c) high AD were shown in low magnification (300 μm) with higher magnification (60 μm) images of GFAP+ NP and GFAP− non-NP on the side. NP and non-NP are defined by the presence of Gallyas Silver staining+ dystrophic neurite (black) around anti-amyloid-β antibody Ab5 (Pink). GFAP+ astrocytic clustering is defined by the presence of GFAP+ cells (brown) around non-NP and NP. (d) Quantification of GFAP+ astrocytic clustering around non-NP and NP in frontal cortex from different ADNC− low AD (n = 5 cases), intermediate AD (n = 7 cases), and high AD (n = 17 cases). GFAP+ astrocytic clustering is significantly higher in NP compared to non-NP in intermediate AD cases (p-value = 0.0156) and high AD cases (p-value < 0.0001). Hippocampus (e–h). Hippocampus images from (e) low AD, (f) intermediate AD, and (g) high AD were shown in low magnification (300 μm) with higher magnification (60 μm) images of GFAP+ NP and GFAP− non-NP on the side. (h) Quantification of GFAP+ astrocytic clustering around non-NP and NP in hippocampal regions from low AD cases (n = 4 cases), intermediate AD cases (n = 10 cases) and high AD cases (20 cases). GFAP+ astrocytic clustering is significantly higher around NP in intermediate AD (p-value = 0.0039) and high AD (p-value = 0.0002). In low AD cases, there is no significant differences but trend toward higher clustering around NP. Data are presented as mean with SD. Shapiro–Wilk test was run to test the normality of data. Wilcoxon matched-pairs signed rank test (two-tailed) was used to compare the percent differences in IBA1+ microglial clustering between non-NP and NP. *p < 0.05, **p < 0.01, ***p < 0.001, ****p < 0.0001.
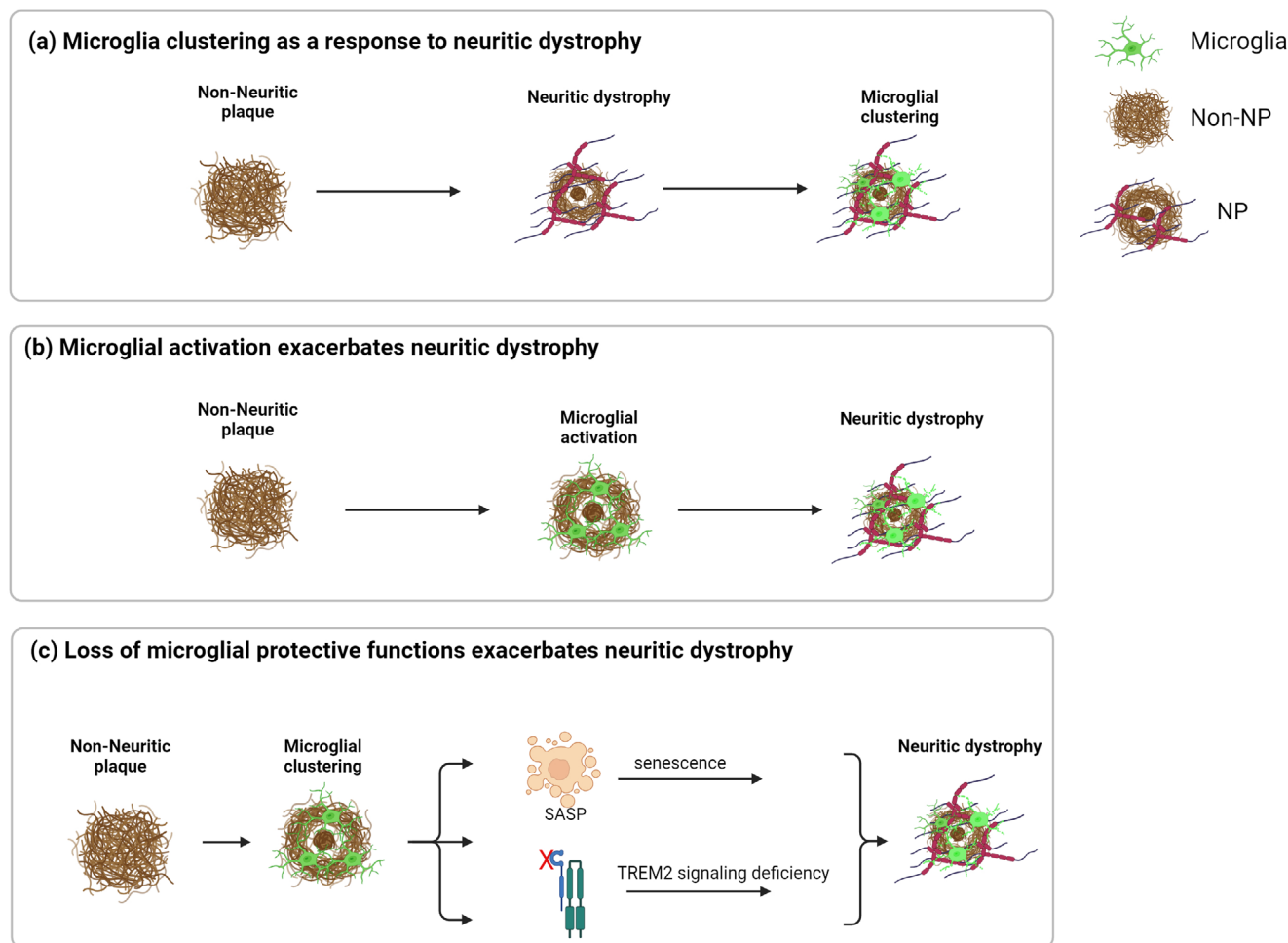
(a) Microglia clustering as a response to neuritic dystrophy

Non-Neuritic plaque → Neuritic dystrophy → Microglial clustering

(b) Microglial activation exacerbates neuritic dystrophy

Non-Neuritic plaque → Microglial activation → Neuritic dystrophy

(c) Loss of microglial protective functions exacerbates neuritic dystrophy

Non-Neuritic plaque → Microglial clustering → SASP → senescence / TREM2 signaling deficiency → Neuritic dystrophy

Microglia · Non-NP · NP

FIGURE 6 Possible relationships between microglial clustering and neuritic dystrophy. In our study, microglia preferentially cluster around neuritic plaques (NP) compared to non-NP. Possible mechanisms of the relationship between neuritic dystrophy and microglial activation and clustering are: (a) amyloid-β (Aβ) plaque causes cytoskeleton alterations around neurons in the form of neuritic dystrophy, and microglia respond to the neuritic damage as a protective mechanism. In this scenario, neuritic dystrophy because of Aβ plaque precedes microglial activation. (b) Microglial activation in response to Aβ plaque exacerbates the neuritic dystrophy. In this scenario, microglial activation precedes the neuritic dystrophy. (c) Microglia respond to the Aβ plaque and cluster around it as a protective mechanism in the early stages of the disease. Over time, when Aβ plaque reaches a threshold, microglia are overwhelmed either because of senescence or TREM2 signaling deficiency, leading to exacerbation of neuritic dystrophy. In this scenario, microglial activation precedes the neuritic dystrophy but the loss of the microglial functions, rather than microglial activation exacerbates the neuritic dystrophy. Created by BioRender.com.

non-NP in the hippocampus. In addition, we noted that the number of microglia of different activation states per plaque is higher in the hippocampus, compared to the frontal cortex. These brain region-specific differences in microglia clustering around Aβ plaques are very interesting considering our previous observation that NP precedes NFT formation in the cortex but not in the hippocampus (Tsering et al., 2023) and may further substantiate the idea of brain region-specific differences in the interaction of Aβ and tau. An alternative explanation for this phenomenon is brain region-specific differences in microglia density and activation status, which have been reported mainly in animal models (Edler et al., 2021; Grabert et al., 2016; Silvin & Ginhoux, 2018).

Overall, our study demonstrates that microglia positive for markers of phagocytosis (CD68), disease-specific activation (CD11c), and

dystrophy (Ferritin) as well as astrocytes are preferentially clustered in and around NP compared to non-NP during the progression of ADNC and highlights brain region-specific differences in this response for microglia, but not astrocytes, which may provide important insights into the brain region-specific interaction between Aβ and tau.

4.1 | Limitations of the study

Our study is cross-sectional and only allows limited conclusion as to a temporal sequence of events. Given the large variety of different morphological types of Aβ deposits our dichotomous distinction between non-NP and NP may overlook important morphological plaque subtypes. We used 8-μm thick tissue sections which may not

completely reflect the spatial orientation of microglia around globular Aβ deposits. Lastly, we only focused on a limited set of microglia markers potentially not capturing the full spectrum of microglia reactivity, although our results using the pan-microglia marker Iba1 are comparable to our results with microglia activation markers.

AUTHOR CONTRIBUTIONS

Wangchen Tsering: Conceptualization; data curation; formal analysis; investigation; methodology; writing – original draft; writing – review and editing. **Ana de la Rosa:** Data curation; methodology. **Isabelle Y. Ruan:** Data curation; methodology. **Jennifer L. Philips:** Data curation; formal analysis; methodology. **Tim Bathe:** Data curation; formal analysis; investigation; methodology. **Jonathan A. Villareal:** Data curation; formal analysis; investigation; methodology. **Stefan Prokop:** Conceptualization; data curation; formal analysis; funding acquisition; investigation; methodology; project administration; writing – review and editing.

CONFLICT OF INTEREST STATEMENT

The authors declare no conflict of interest.

PEER REVIEW

The peer review history for this article is available at https://www.webofscience.com/api/gateway/wos/peer-review/10.1111/jnc.16275.

DATA AVAILABILITY STATEMENT

The data that support the findings of this study are available upon request.

ORCID

Wangchen Tsering https://orcid.org/0000-0002-3271-1128
Tim Bathe https://orcid.org/0000-0001-9824-2064
Jonathan A. Villareal https://orcid.org/0009-0008-9450-4520
Stefan Prokop https://orcid.org/0000-0002-5633-2149

REFERENCES

Bai, B., Wang, X., Li, Y., Chen, P. C., Yu, K., Dey, K. K., Yarbro, J. M., Han, X., Lutz, B. M., Rao, S., Jiao, Y., Sifford, J. M., Han, J., Wang, M., Tan, H., Shaw, T. I., Cho, J. H., Zhou, S., Wang, H., ... Peng, J. (2020). Deep multilayer brain proteomics identifies molecular networks in Alzheimer's disease progression. *Neuron*, *105*(6), 975–991.e7. https://doi.org/10.1016/j.neuron.2019.12.015

Bankhead, P., Loughrey, M. B., Fernández, J. A., Dombrowski, Y., McArt, D. G., Dunne, P. D., McQuaid, S., Gray, R. T., Murray, L. J., Coleman, H. G., James, J. A., Salto-Tellez, M., & Hamilton, P. W. (2017). QuPath: Open source software for digital pathology image analysis. *Scientific Reports*, *7*(1), 1–7. https://doi.org/10.1038/s41598-017-17204-5

Bathe, T., Hery, G. P., Villareal, J. A. B., Phillips, J. L., Cohen, E. M., Sharma, R. V., Tsering, W., & Prokop, S. (2024). Disease and brain region specific immune response profiles in neurodegenerative diseases with pure and mixed protein pathologies. *Acta Neuropathologica Communications*, *12*(1), 1–25. https://doi.org/10.1186/S40478-024-01770-7

Boon, B. D. C., Bulk, M., Jonker, A. J., Morrema, T. H. J., van den Berg, E., Popovic, M., Walter, J., Kumar, S., van der Lee, S. J., Holstege, H., Zhu, X., Van Nostrand, W. E., Natté, R., van der Weerd, L., Bouwman, F. H., van de Berg, W. D. J., Rozemuller, A. J. M., & Hoozemans, J. J. M. (2020). The coarse-grained plaque: A divergent Aβ plaque-type in early-onset Alzheimer's disease. *Acta Neuropathologica*, *140*(6), 811–830. https://doi.org/10.1007/s00401-020-02198-8

Busch, S. A., & Silver, J. (2007). The role of extracellular matrix in CNS regeneration. *Current Opinion in Neurobiology*, *17*, 120–127. https://doi.org/10.1016/j.conb.2006.09.004

Choi, I., Wang, M., Yoo, S., Xu, P., Seegobin, S. P., Li, X., Han, X., Wang, Q., Peng, J., Zhang, B., & Yue, Z. (2023). Autophagy enables microglia to engage amyloid plaques and prevents microglial senescence. *Nature Cell Biology*, *25*(7), 963–974. https://doi.org/10.1038/S41556-023-01158-0

Crook, R., Verkkoniemi, A., Perez-Tur, J., Mehta, N., Baker, M., Houlden, H., Farrer, M., Hutton, M., Lincoln, S., Hardy, J., Gwinn, K., Somer, M., Paetau, A., Kalimo, H., Ylikoski, R., Pöyhönen, M., Kucera, S., & Haltia, M. (1998). A variant of Alzheimer's disease with spastic paraparesis and unusual plaques due to deletion of exon 9 of presenilin 1. *Nature Medicine*, *4*(4), 452–455. https://doi.org/10.1038/nm0498-452

De Strooper, B., & Karran, E. (2016). The cellular phase of Alzheimer's disease. *Cell*, *164*(4), 603–615. https://doi.org/10.1016/j.cell.2015.12.056

Del-Aguila, J. L., Li, Z., Dube, U., Mihindukulasuriya, K. A., Budde, J. P., Fernandez, M. V., Ibanez, L., Bradley, J., Wang, F., Bergmann, K., Davenport, R., Morris, J. C., Holtzman, D. M., Perrin, R. J., Benitez, B. A., Dougherty, J., Cruchaga, C., & Harari, O. (2019). A single-nuclei RNA sequencing study of Mendelian and sporadic AD in the human brain. *Alzheimer's Research & Therapy*, *11*(1), 71. https://doi.org/10.1186/S13195-019-0524-X

Delizannis, A. T., Nonneman, A., Tsering, W., De Bondt, A., Van den Wyngaert, I., Zhang, B., Meymand, E., Olufemi, M. F., Koivula, P., Maimaiti, S., Trojanowski, J. Q., Lee, V. M.-Y., & Brunden, K. R. (2021). Effects of microglial depletion and TREM2 deficiency on Aβ plaque burden and neuritic plaque tau pathology in 5XFAD mice. *Acta Neuropathologica Communications*, *9*(1), 150. https://doi.org/10.1186/s40478-021-01251-1

Dewitt, D. A., & Silver, J. (1996). Regenerative failure: A potential mechanism for neuritic dystrophy in Alzheimer's disease. *Experimental Neurology*, *142*(1), 103–110. https://doi.org/10.1006/EXNR.1996.0182

Dickson, T. C., & Vickers, J. C. (2001). The morphological phenotype of β-amyloid plaques and associated neuritic changes in Alzheimer's disease. *Neuroscience*, *105*(1), 99–107. https://doi.org/10.1016/s0306-4522(01)00169-5

Edler, M. K., Mhatre-Winters, I., & Richardson, J. R. (2021). Microglia in aging and Alzheimer's disease: A comparative species review. *Cells*, *10*(5), 1138. https://doi.org/10.3390/CELLS10051138

Fasnacht, J. S., Wueest, A. S., Berres, M., Thomann, A. E., Krumm, S., Gutbrod, K., Steiner, L. A., Goettel, N., & Monsch, A. U. (2023).

14 of 15 | **WILEY**— Journal of Neurochemistry JNC The Official Journal of the International Society for Neurochemistry

TSERING ET AL.

Conversion between the Montreal cognitive assessment and the mini-mental status examination. *Journal of the American Geriatrics Society, 71*(3), 869–879. https://doi.org/10.1111/JGS.18124

Fitch, M. T., & Silver, J. (2008). CNS injury, glial scars, and inflammation: Inhibitory extracellular matrices and regeneration failure. *Experimental Neurology, 209*(2), 294–301. https://doi.org/10.1016/J.EXPNEUROL.2007.05.014

Grabert, K., Michoel, T., Karavolos, M. H., Clohisey, S. J., Baillie, K., Stevens, M. P., Freeman, T. C., Summers, K. M., & Mccoll, B. W. (2016). Microglial brain region–dependent diversity and selective regional sensitivities to aging. *Nature Neuroscience, 19*, 504–516. https://doi.org/10.1038/nn.4222

Gratuze, M., Chen, Y., Parhizkar, S., Jain, N., Strickland, M. R., Serrano, J. R., Colonna, M., Ulrich, J. D., & Holtzman, D. M. (2021). Activated microglia mitigate aβ-associated tau seeding and spreading. *Journal of Experimental Medicine, 218*(8), e20210542. https://doi.org/10.1084/JEM.20210542/212263

Hardy, J., & Selkoe, D. J. (2002). The amyloid hypothesis of Alzheimer's disease: Progress and problems on the road to therapeutics. *Science, 297*(5580), 353–356. https://doi.org/10.1126/science.1072994

Hardy, J. A., & Higgins, G. A. (1992). Alzheimer's disease: The amyloid cascade hypothesis. *Science, 256*(5054), 184–185. https://doi.org/10.1126/SCIENCE.1566067/ASSET/74A758CB-215F-4A8E-9AAA-05F4D89DA62A/ASSETS/SCIENCE.1566067.FP.PNG

Hendrickx, D. A. E., van Eden, C. G., Schuurman, K. G., Hamann, J., & Huitinga, I. (2017). Staining of HLA-DR, Iba1 and CD68 in human microglia reveals partially overlapping expression depending on cellular morphology and pathology. *Journal of Neuroimmunology, 309*, 12–22. https://doi.org/10.1016/j.jneuroim.2017.04.007

Hopperton, K. E., Mohammad, D., Trépanier, M. O., Giuliano, V., & Bazinet, R. P. (2018). Markers of microglia in post-mortem brain samples from patients with Alzheimer's disease: A systematic review. *Molecular Psychiatry, 23*(2), 177–198. https://doi.org/10.1038/MP.2017.246

Jia, J., Ning, Y., Chen, M., Wang, S., Yang, H., Li, F., Ding, J., Li, Y., Zhao, B., Lyu, J., Yang, S., Yan, X., Wang, Y., Qin, W., Wang, Q., Li, Y., Zhang, J., Liang, F., Liao, Z., & Wang, S. (2024). Biomarker changes during 20 years preceding Alzheimer's disease. *The New England Journal of Medicine, 390*(8), 712–722. https://doi.org/10.1056/NEJMOA2310168

Johnson, E. C. B., Carter, E. K., Dammer, E. B., Duong, D. M., Gerasimov, E. S., Liu, Y., Liu, J., Betarbet, R., Ping, L., Yin, L., Serrano, G. E., Beach, T. G., Peng, J., De Jager, P. L., Haroutunian, V., Zhang, B., Gaiteri, C., Bennett, D. A., Gearing, M., ... Seyfried, N. T. (2022). Large-scale deep multi-layer analysis of Alzheimer's disease brain reveals strong proteomic disease-related changes not observed at the RNA level. *Nature Neuroscience, 25*(2), 213–225. https://doi.org/10.1038/s41593-021-00999-y

Jury-Garfe, N., Redding-Ochoa, J., You, Y., Martínez, P., Karahan, H., Chimal-Juárez, E., Johnson, T. S., Zhang, J., Resnick, S., Kim, J., Troncoso, J. C., & Lasagna-Reeves, C. A. (2024). Enhanced microglial dynamics and a paucity of tau seeding in the amyloid plaque microenvironment contribute to cognitive resilience in Alzheimer's disease. *Acta Neuropathologica, 148*, 15. https://doi.org/10.1007/s00401-024-02775-1

Keren-Shaul, H., Spinrad, A., Weiner, A., Matcovitch-Natan, O., Dvir-Szternfeld, R., Ulland, T. K., David, E., Baruch, K., Lara-Astaiso, D., Toth, B., Itzkovitz, S., Colonna, M., Schwartz, M., & Amit, I. (2017). A unique microglia type associated with restricting development of Alzheimer's disease. *Cell, 169*(7), 1276–1290.e17. https://doi.org/10.1016/J.CELL.2017.05.018

Khakh, B. S., & Sofroniew, M. V. (2015). Diversity of astrocyte functions and phenotypes in neural circuits. *Nature Neuroscience, 18*(7), 942–952. https://doi.org/10.1038/nn.4043

Levites, Y., Dammer, E. B., Ran, Y., Tsering, W., Duong, D., Abreha, M., Gadhavi, J., Lolo, K., Trejo-Lopez, J., Phillips, J., Iturbe, A., Erquizi, A., Moore, B. D., Ryu, D., Natu, A., Dillon, K., Torrellas, J., Moran, C., Ladd, T., ... Golde, T. E. (2024). Integrative proteomics identifies a conserved Aβ amyloid responsome, novel plaque proteins, and pathology modifiers in Alzheimer's disease. *Cell Reports Medicine, 5*, 101669. https://doi.org/10.1016/J.XCRM.2024.101669

Leyns, C. E. G., Gratuze, M., Narasimhan, S., Jain, N., Koscal, L. J., Jiang, H., Manis, M., Colonna, M., Lee, V. M. Y., Ulrich, J. D., & Holtzman, D. M. (2019). TREM2 function impedes tau seeding in neuritic plaques. *Nature Neuroscience, 22*(8), 1217–1222. https://doi.org/10.1038/s41593-019-0433-0

Li, Y., Yen, D., Hendrix, R. D., Gordon, B. A., Dlamini, S., Barthélemy, N. R., Aschenbrenner, A. J., Henson, R. L., Herries, E. M., Volluz, K., Kirmess, K., Eastwood, S., Meyer, M., Heller, M., Jarrett, L., McDade, E., Holtzman, D. M., Benzinger, T. L. S., Morris, J. C., ... Schindler, S. E. (2024). Timing of biomarker changes in sporadic Alzheimer's disease in estimated years from symptom onset. *Annals of Neurology, 95*, 951–965. https://doi.org/10.1002/ANA.26891

Liddelow, S. A., Guttenplan, K. A., Clarke, L. E., Bennett, F. C., Bohlen, C. J., Schirmer, L., Bennett, M. L., Münch, A. E., Chung, W. S., Peterson, T. C., Wilton, D. K., Frouin, A., Napier, B. A., Panicker, N., Kumar, M., Buckwalter, M. S., Rowitch, D. H., Dawson, V. L., Dawson, T. M., ... Barres, B. A. (2017). Neurotoxic reactive astrocytes are induced by activated microglia. *Nature, 541*(7638), 481–487. https://doi.org/10.1038/nature21029

Lopes, K. O., Sparks, D. L., & Streit, W. J. (2008). Microglial dystrophy in the aged and Alzheimer's disease brain is associated with ferritin immunoreactivity. *Glia, 56*(10), 1048–1060. https://doi.org/10.1002/glia.20678

Mancuso, R., Fattorelli, N., Martinez-Muriana, A., Davis, E., Wolfs, L., Van Den Daele, J., Geric, I., Premereur, J., Polanco, P., Bijnens, B., Preman, P., Serneels, L., Poovathingal, S., Balusu, S., Verfaillie, C., Fiers, M., & De Strooper, B. (2024). Xenografted human microglia display diverse transcriptomic states in response to Alzheimer's disease-related amyloid-β pathology. *Nature Neuroscience, 2024*, 1–15. https://doi.org/10.1038/s41593-024-01600-y

Mathys, H., Davila-Velderrain, J., Peng, Z., Gao, F., Mohammadi, S., Young, J. Z., Menon, M., He, L., Abdurrob, F., Jiang, X., Martorell, A. J., Ransohoff, R. M., Hafler, B. P., Bennett, D. A., Kellis, M., & Tsai, L. H. (2019). Single-cell transcriptomic analysis of Alzheimer's disease. *Nature, 570*(7761), 332–337. https://doi.org/10.1038/S41586-019-1195-2

Matias, I., Morgado, J., & Gomes, F. C. A. (2019). Astrocyte heterogeneity: Impact to brain aging and disease. *Frontiers in Aging Neuroscience, 11*, 447123. https://doi.org/10.3389/FNAGI.2019.00059/BIBTEX

McGeer, P. L., & McGeer, E. G. (2013). The amyloid cascade-inflammatory hypothesis of Alzheimer disease: Implications for therapy. *Acta Neuropathologica, 126*(4), 479–497. https://doi.org/10.1007/S00401-013-1177-7

Montine, T. J., Phelps, C. H., Beach, T. G., Bigio, E. H., Cairns, N. J., Dickson, D. W., Duyckaerts, C., Frosch, M. P., Masliah, E., Mirra, S. S., Nelson, P. T., Schneider, J. A., Thal, D. R., Trojanowski, J. Q., Vinters, H. V., & Hyman, B. T. (2012). National Institute on Aging-Alzheimer's Association guidelines for the neuropathologic assessment of Alzheimer's disease: A practical approach. *Acta Neuropathologica, 123*(1), 1–11. https://doi.org/10.1007/S00401-011-0910-3

Ohgami, T., Kitamoto, T., Shin, R. W., Kaneko, Y., Ogomori, K., & Tateishi, J. (1991). Increased senile plaques without microglia in Alzheimer's disease. *Acta Neuropathologica, 81*(3), 242–247. https://doi.org/10.1007/bf00305864

Paasila, P. J., Davies, D. S., Kril, J. J., Goldsbury, C., & Sutherland, G. T. (2019). The relationship between the morphological subtypes of microglia and Alzheimer's disease neuropathology. *Brain Pathology, 29*(6), 726–740. https://doi.org/10.1111/BPA.12717

Paasila, P. J., Davies, D. S., Sutherland, G. T., & Goldsbury, C. (2020). Clustering of activated microglia occurs before the formation of dystrophic neurites in the evolution of Aβ plaques in Alzheimer's disease. *Free Neuropathology, 1*, 20. https://doi.org/10.17879/FREENEUROPATHOLOGY-2020-2845

Prokop, S., Lee, V. M. Y., & Trojanowski, J. Q. (2019). Neuroimmune interactions in Alzheimer's disease-new frontier with old challenges? *Progress in Molecular Biology and Translational Science*, *168*, 183–201. https://doi.org/10.1016/BS.PMBTS.2019.10.002

Prokop, S., Miller, K. R., & Heppner, F. L. (2013). Microglia actions in Alzheimer's disease. *Acta Neuropathologica*, *126*(4), 461–477. https://doi.org/10.1007/S00401-013-1182-X/TABLES/1

Prokop, S., Miller, K. R., Labra, S. R., Pitkin, R. M., Hoxha, K., Narasimhan, S., Changolkar, L., Rosenbloom, A., Lee, V. M. Y., & Trojanowski, J. Q. (2019). Impact of TREM2 risk variants on brain region-specific immune activation and plaque microenvironment in Alzheimer's disease patient brain samples. *Acta Neuropathologica*, *138*(4), 613–630. https://doi.org/10.1007/S00401-019-02048-2

Schindelin, J., Arganda-Carreras, I., Frise, E., Kaynig, V., Longair, M., Pietzsch, T., Preibisch, S., Rueden, C., Saalfeld, S., Schmid, B., Tinevez, J. Y., White, D. J., Hartenstein, V., Eliceiri, K., Tomancak, P., & Cardona, A. (2012). Fiji: An open-source platform for biological-image analysis. *Nature Methods*, *9*(7), 676–682. https://doi.org/10.1038/nmeth.2019

Selkoe, D. J., & Hardy, J. (2016). The amyloid hypothesis of Alzheimer's disease at 25 years. *EMBO Molecular Medicine*, *8*(6), 595–608. https://doi.org/10.15252/emmm.201606210

Serrano-Pozo, A., Muzikansky, A., Gómez-Isla, T., Growdon, J. H., Betensky, R. A., Frosch, M. P., & Hyman, B. T. (2013). *Differential relationships of reactive astrocytes and microglia to fibrillar amyloid deposits in Alzheimer disease*. https://academic.oup.com/jnen/article-abstract/72/6/462/2917518

Shahidehpour, R. K., Nelson, P. T., Katsumata, Y., & Bachstetter, A. D. (2012). Exploring the link between dystrophic microglia and the spread of Alzheimer's neuropathology. *Brain*, *139*(4), 16–17. https://doi.org/10.1093/BRAIN/AWAE258

Silvin, A., & Ginhoux, F. (2018). Microglia heterogeneity along a spatiotemporal axis: More questions than answers. *Glia*, *66*, 2045–2057. https://doi.org/10.1002/glia.23458

Sofroniew, M. V., & Vinters, H. V. (2009). Astrocytes: Biology and pathology. *Acta Neuropathologica*, *119*, 7–35. https://doi.org/10.1007/s00401-009-0619-8

Sosna, J., Philipp, S., Albay, R., 3rd, Reyes-Ruiz, J. M., Baglietto-Vargas, D., LaFerla, F. M., & Glabe, C. G. (2018). Early long-term administration of the CSF1R inhibitor PLX3397 ablates microglia and reduces accumulation of intraneuronal amyloid, neuritic plaque deposition and pre-fibrillar oligomers in 5XFAD mouse model of Alzheimer's disease. *Molecular Neurodegeneration*, *13*(1), 11. https://doi.org/10.1186/s13024-018-0244-x

Spangenberg, E., Severson, P. L., Hohsfield, L. A., Crapser, J., Zhang, J., Burton, E. A., Zhang, Y., Spevak, W., Lin, J., Phan, N. Y., Habets, G., Rymar, A., Tsang, G., Walters, J., Nespi, M., Singh, P., Broome, S., Ibrahim, P., Zhang, C., … Green, K. N. (2019). Sustained microglial depletion with CSF1R inhibitor impairs parenchymal plaque development in an Alzheimer's disease model. *Nature Communications*, *10*(1), 1–21. https://doi.org/10.1038/s41467-019-11674-z

Srinivasan, K., Friedman, B. A., Etxeberria, A., Huntley, M. A., van der Brug, M. P., Foreman, O., Paw, J. S., Modrusan, Z., Beach, T. G., Serrano, G. E., & Hansen, D. V. (2020). Alzheimer's patient microglia exhibit enhanced aging and unique transcriptional activation. *Cell Reports*, *31*(13), 107843. https://doi.org/10.1016/J.CELREP.2020.107843

Streit, W. J., Braak, H., Xue, Q. S., & Bechmann, I. (2009). Dystrophic (senescent) rather than activated microglial cells are associated with tau pathology and likely precede neurodegeneration in Alzheimer's disease. *Acta Neuropathologica*, *118*(4), 475–485. https://doi.org/10.1007/S00401-009-0556-6/FIGURES/7

Streit, W. J., Khoshbouei, H., & Bechmann, I. (2021). The role of microglia in sporadic Alzheimer's disease. *Journal of Alzheimer's Disease*, *79*(3), 961–968. https://doi.org/10.3233/JAD-201248

Trejo-Lopez, J. A., Yachnis, A. T., & Prokop, S. (2022). Neuropathology of Alzheimer's disease. *Neurotherapeutics*, *19*(1), 173–185. https://doi.org/10.1007/s13311-021-01146-y

Tsering, W., Hery, G. P., Phillips, J. L., Lolo, K., Bathe, T., Villareal, J. A., Ruan, I. Y., & Prokop, S. (2023). Transformation of non-neuritic into neuritic plaques during AD progression drives cortical spread of tau pathology via regenerative failure. *Acta Neuropathologica Communications*, *11*(1), 1–20. https://doi.org/10.1186/S40478-023-01688-6/FIGURES/7

Tsering, W., & Prokop, S. (2023). Neuritic plaques—Gateways to understanding Alzheimer's disease. *Molecular Neurobiology*, *2023*(1), 1–14. https://doi.org/10.1007/S12035-023-03736-7

Wang, Y., Ulland, T. K., Ulrich, J. D., Song, W., Tzaferis, J. A., Hole, J. T., Yuan, P., Mahan, T. E., Shi, Y., Gilfillan, S., Cella, M., Grutzendler, J., DeMattos, R. B., Cirrito, J. R., Holtzman, D. M., & Colonna, M. (2016). TREM2-mediated early microglial response limits diffusion and toxicity of amyloid plaques. *Journal of Experimental Medicine*, *213*(5), 667–675. https://doi.org/10.1084/jem.20151948

Wlodarczyk, A., Holtman, I. R., Krueger, M., Yogev, N., Bruttger, J., Khorooshi, R., Benmamar-Badel, A., De Boer-Bergsma, J. J., Martin, N. A., Karram, K., Kramer, I., Wgm Boddeke, E., Waisman, A., Jl Eggen, B., & Owens, T. (2017). A novel microglial subset plays a key role in myelinogenesis in developing brain. *The EMBO Journal*, *36*, 3292–3308. https://doi.org/10.15252/embj.201696056

Xia, Y., Prokop, S., Gorion, K. M., Kim, J. D., Sorrentino, Z. A., Bell, B. M., Manaois, A. N., Chakrabarty, P., Davies, P., & Giasson, B. I. (2020). Tau Ser208 phosphorylation promotes aggregation and reveals neuropathologic diversity in Alzheimer's disease and other tauopathies. *Acta Neuropathologica Communications*, *8*(1), 88. https://doi.org/10.1186/S40478-020-00967-W

Xu, G., Fromholt, S. E., Chakrabarty, P., Zhu, F., Liu, X., Pace, M. C., Koh, J., Golde, T. E., Levites, Y., Lewis, J., & Borchelt, D. R. (2020). Diversity in Aβ deposit morphology and secondary proteome insolubility across models of Alzheimer-type amyloidosis. *Acta Neuropathologica Communications*, *8*(1), 43. https://doi.org/10.1186/S40478-020-00911-Y

Yuan, P., Condello, C., Keene, C. D., Wang, Y., Bird, T. D., Paul, S. M., Luo, W., Colonna, M., Baddeley, D., & Grutzendler, J. (2016). TREM2 haplodeficiency in mice and humans impairs the microglia barrier function leading to decreased amyloid compaction and severe axonal dystrophy. *Neuron*, *90*(4), 724–739. https://doi.org/10.1016/J.NEURON.2016.05.003

Yuan, Q., Su, H., Zhang, Y., Chau, W. H., Ng, C. T., Wu, W., & Lin, Z. X. (2013). Existence of different types of senile plaques between brain and spinal cord of TgCRND8 mice. *Neurochemistry International*, *62*(3), 211–220. https://doi.org/10.1016/J.NEUINT.2013.01.006

Zeng, H., Huang, J., Zhou, H., Meilandt, W. J., Dejanovic, B., Zhou, Y., Bohlen, C. J., Lee, S. H., Ren, J., Liu, A., Tang, Z., Sheng, H., Liu, J., Sheng, M., & Wang, X. (2023). Integrative in situ mapping of single-cell transcriptional states and tissue histopathology in a mouse model of Alzheimer's disease. *Nature Neuroscience*, *26*(3), 430–446. https://doi.org/10.1038/S41593-022-01251-X

SUPPORTING INFORMATION

Additional supporting information can be found online in the Supporting Information section at the end of this article.